Initiation Efficiency in the Synthesis of Molecular Brushes by Grafting from via Atom Transfer Radical Polymerization

Brent S. Sumerlin, Dorota Neugebauer,† and Krzysztof Matyjaszewski*

Center for Macromolecular Engineering, Department of Chemistry, Carnegie Mellon University, 4400 Fifth Avenue, Pittsburgh, Pennsylvania 15213

Received August 10, 2004; Revised Manuscript Received November 13, 2004

ABSTRACT: Grafting from via atom transfer radical polymerization (ATRP) was employed for the synthesis of densely grafted molecular brushes. A poly(2-(2-bromopropionyl)oxyethyl methacrylate) (PBPEM) macroinitiator was used to polymerize *n*-butyl acrylate (BA) with various degrees of polymerization. The brush syntheses proceeded with first-order kinetic behavior, and the molecular weights determined by gel permeation chromatography coupled with multiangle laser light scattering (GPC-MALLS) increased linearly with conversion. The PBA side chains (SCs) were cleaved by acid solvolysis, and the resulting products were characterized in order to study the initiation process in the synthesis of molecular brushes. By comparing the molecular weight of the cleaved SCs to their theoretical molecular weights (calculated assuming quantitative initiation), the grafting efficiency was determined as a function of monomer conversion. In the early stages of polymerization, the initiation efficiency is low but gradually increases to 87% at 12% monomer conversion. The results were compared to an analogous linear ATRP conducted under identical conditions, except that ethyl 2-bromopropionate was employed as the initiator. The initiation efficiency for the linear polymerization was consistently higher than that observed for the brushes. The difference was attributed to the congested environment (high local concentration of initiation sites) encountered in the case of grafting from a macroinitiator backbone, which led to slower deactivation of growing radicals at low conversion. The initiation efficiency was enhanced by increasing the rate of deactivation of the growing species or decreasing the rate of propagation.

Introduction

Molecular brushes are a specific class of graft copolymers[1] containing a high density of side chains (SCs) that are separated by a distance that is much less than their unperturbed dimensions. This leads to significant congestion and entropically unfavorable extension of the backbone and SCs, which prevents the polymer from adopting a random coil conformation.[2] Instead, the persistence length of the polymer is forced to approach the dimensions of the extended backbone. This gives rise to polymers with interesting properties as observed in bulk,[3] in solution,[2,4,5] and at interfaces.[6−12]

Three main approaches have been employed for the synthesis of macromolecular brushes: "grafting to",[13−16] "grafting through",[17,18] and "grafting from".[4,6,7,19] Grafting to involves the attachment of a living or telechelic polymer to a separately prepared backbone polymer that contains reactive functional groups along its chain. This approach is beneficial because it allows the individual synthesis and characterization of the backbone and SCs; however, the grafting density is limited since attachment becomes progressively more difficult with increasing conversion and/or SC length due to steric congestion. An excess of the reactive SC must be employed leading to further difficulties in purification, which must be accomplished by fractionation.

The grafting through route involves the synthesis of macromonomers−polymers with polymerizable end groups. Several polymerization mechanisms have proven successful, including anionic,[5,20,21] free radical,[22] controlled/living free radical,[11,18] and ring-opening metathesis.[23,24] Grafting through ensures SC attachment to every backbone unit, but this method suffers from the degree of polymerization of the backbone being dependent on the macromonomer length and type.[18] Again, purification is difficult for this method as well since it also requires fractionation to remove unreacted macromonomer.

Grafting from involves the preparation of a backbone polymer (macroinitiator) with a predetermined number of initiation sites that is subsequently used to initiate polymerization. High molecular weight backbones can be used, and the grafting density is not adversely affected with increasing monomer conversion. There have been several reports of molecular brush synthesis by grafting from via atom transfer radical polymerization (ATRP) of styrenic,[4,6,7] acrylate,[4,6,7] and methacrylate[11] monomers. ATRP and other controlled radical polymerization mechanisms are suitable for molecular brush synthesis since they facilitate low radical concentrations which causes inter- and intramolecular termination events to be significantly suppressed.[21,25−27] This is especially important for brush polymerizations due to the high local concentration of chains that exist in the vicinity of the backbone polymer.

When considering brush synthesis by any of the above-mentioned routes, it is important to understand the fundamentals that affect grafting density since this is largely responsible for the resulting unique material properties. Because of the high local concentration of initiation sites present on the backbone, steric interactions may adversely affect the efficiency of the grafting process. This would also affect the uniformity (polydispersity) of the resulting SCs and possibly limit the ability to prepare well-defined core−shell molecules with block copolymer SCs. Herein, we study the initia-

† Permanent address: Centre of Polymer Chemistry, PASci., 41-819 Zabrze, Poland.

* Corresponding author. E-mail: km3b@andrew.cmu.edu.

10.1021/ma048351b CCC: $30.25
Published on Web 01/14/2005

Table 1. Molar Ratios of Reagents for the Atom Transfer Radical Polymerization of *n*-Butyl Acrylate (BA) from a Poly(2-(2-bromopropionyl)oxyethyl methacrylate) (PBPEM) Macroinitiator (B1−3) and Ethyl 2-Bromopropionate (EtBrP) (L1)

	[BA]	[R−Br][a]	[CuBr]	[$CuBr_2$]	[dNbpy][b]	toluene (vol %)
L1	400	1	0.5	0.025	1	0
B1	400	1	0.5	0.025	1	0
B2	400	1	2.5	0.125	5	0
B3	200	0.5	0.5	0.025	1	50

[a] Where R = $EtOOCCH(CH_3)$ for **L1** and R = BPEM for **B1−3**. [b] dNbpy = 4,4′-di(5-nonyl)-2,2′-bipyridine.

tion efficiency for the ATRP of *n*-butyl acrylate (BA) from a poly(2-(2-bromopropionyl)oxyethyl methacrylate) (PBPEM) macroinitiator. To isolate the effects of the congested environment on the initiation process, the results are compared to those obtained during an analogous linear polymerization of BA initiated with a similar low molar mass ATRP initiator. Two methods are discussed for improving the initiation efficiency of the brush polymerization at low conversion. These results may not be limited to the synthesis of molecular brushes and could possibly provide valuable insight into the initiation phenomena of polymerizations conducted in other sterically congested environments.

Experimental Section

Materials. All chemicals were purchased from Aldrich and used as received unless otherwise stated. BA and 2-(trimethylsilyloxy)ethyl methacrylate (HEMA-TMS, 99%) were distilled under vacuum prior to use. CuBr (98%) was purified by stirring with glacial acetic acid followed by filtering and washing the resulting solid with ethanol (×3) and diethyl ether (×2). 4,4′-Di(5-nonyl)-2,2′-bipyridine (dNbpy) was prepared as previously reported.[28] 2,2′-Azobis(isobutyronitrile) (AIBN, 98%) was recrystallized twice from ethanol.

Synthesis. Poly(HEMA-TMS) and PBPEM (M_n = 123 000 g/mol, M_w/M_n = 1.15, 97% functionalized) were prepared as previously reported.[6] The general conditions for the brush syntheses are listed in Table 1.

P(BPEM-graft-BA) (**B1**). PBPEM (0.100 g, 0.379 mmol initiating sites), $CuBr_2$ (99%) (0.002 g, 0.009 mmol), dNbpy (0.154 g, 0.377 mmol), BA (99+%) (19.5 g, 0.152 mol), and methyl ethyl ketone (MEK) (1.0 mL) were added to a 50 mL Schlenk flask equipped with a magnetic stir bar. The flask was sealed, and the resulting solution was subjected to three freeze−pump−thaw cycles. After equilibration to room temperature, CuBr (0.0273 g, 0.190 mmol) was added to the solution, and the flask was placed in an oil bath preheated to 70 °C. Aliquots were removed by syringe at regularly spaced intervals in order to monitor conversion and molecular weight evolution. After a predetermined time, the flask was removed from the oil bath and opened to expose to air. The polymerization solution was diluted with $CHCl_3$ and passed over an alumina (activated neutral) column to remove the catalyst. Solvent was removed by rotary evaporation, and the polymer was isolated by vacuum distillation at room temperature. Several polymerizations were conducted with identical conditions but varying reaction times. This facilitated the determination of conversion by GC and gravimetry at various time intervals.

Linear PBA (L1,L2). For an analogous linear polymerization (**L1**), BA was polymerized with conditions identical to those employed for the synthesis of P(BPEM-*graft*-BA), except that ethyl 2-bromopropionate (EtBrP, 99%) was employed as a low molecular weight ATRP initiator. High molecular weight linear PBA (**L2**) was prepared by conventional radical polymerization of BA (5.39 g, 42.1 mmol) in bulk at 60 °C with AIBN (7 mg, 0.04 mmol).

Side Chain Solvolysis. P(BPEM-*graft*-BA) (25 mg) was dissolved in THF (1.5 mL) and 1-butanol (99+%) (8.5 mL). Concentrated sulfuric acid (~3 drops) was added, and the solution was heated at 100 °C for 7 days. The solvent was removed under vacuum, and the remaining residue was dissolved in $CHCl_3$ (4 mL). After extracting with water (1.5 mL), the organic layer was isolated and vacuum-distilled at room temperature. The resulting polymer was characterized by GPC, which indicated nearly quantitative cleavage.

Characterization. Monomer conversion was determined by gravimetry and with a Shimadzu GC 14A gas chromatograph with a flame ionization detector and a J&W Scientific 30 m DB608 column (injector temperature = 250 °C; detector temperature = 250 °C; column initial temperature = 40 °C; heat ramp = 40 °C/min; column final temperature = 190 °C). The degree of functionalization of the macroinitiator was determined by ^1H NMR spectroscopy in $CDCl_3$ with a Bruker Avance DMX-500 spectrometer operating at 500.13 MHz. Absolute and apparent molecular weights were determined by GPC (Waters Microstyragel columns (guard, 10^5, 10^3, and 10^2 Å), THF eluent at 35 °C, flow rate = 1.00 mL/min). The detectors consisted of a differential refractometer (Waters 410, λ = 930 nm) and a multiangle laser light scattering (MALLS) detector (Wyatt Technology DAWN EOS, 30 mW, λ = 690 nm). Apparent molecular weights were determined with a calibration based on poly(methyl methacrylate) (PMMA) or PBA standards using GPCWin software from Polymer Standards Service. Absolute molecular weights were determined with the d*n*/d*c* values[7] of PBPEM (0.084 mL/g) and PBA (0.069 mL/g) using Wyatt ASTRA software.

Results and Discussion

BA was grafted from a PBPEM macroinitiator (M_n = 123 000 (DP_n = 466); PDI = 1.15) to give brushes with several different lengths of SCs (Scheme 1). While there is a range of polymerization variables that can be considered, we employed conditions (temperature, catalyst, initiator concentration) that were previously shown

Scheme 1. Outline for Macroinitiator and Molecular Brush Synthesis

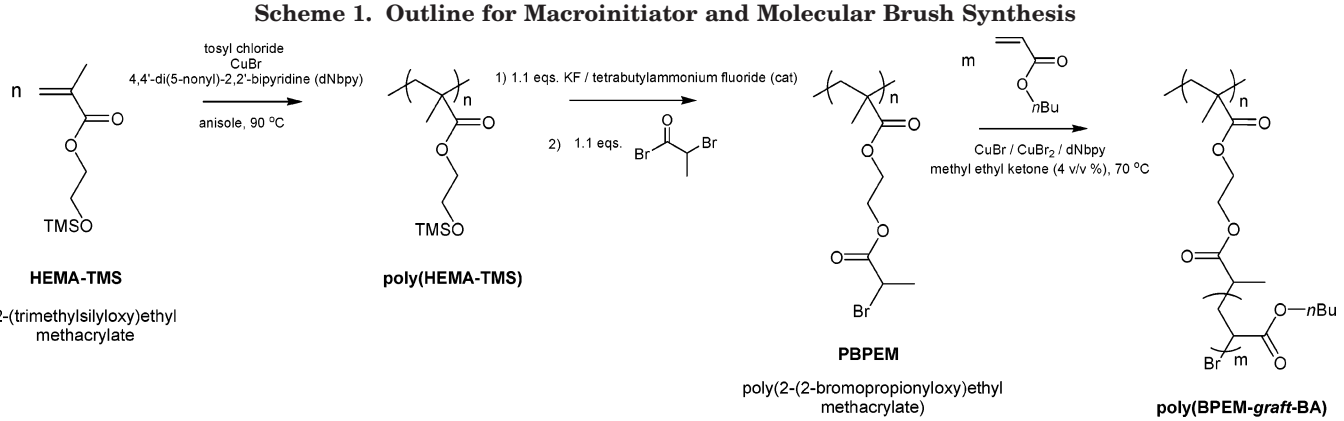

Table 2. Results from Polymerization of *n*-Butyl Acrylate (BA) from a Poly(2-(2-bromopropionyl)oxyethyl methacrylate) (PBPEM) (B1)

time (h)	conv[a] (%)	M_n theory[b]	$DP_{n,SC-theory}$[c]	M_n GPC[d]	M_n GPC-MALLS[e]	SC DP_n	PDI[e]
0	0	123 000		77 200	123 000		1.15
5	1.0	362 000	6	149 500	223 000	2	1.15
20	3.8	1 030 000	4	516 000	998 400	15	1.16
22	5.0	1 316 000	22	603 900	1 292 000	20	1.14
26	6.3	1 626 000	24	778 900	1 592 000	25	1.15
47	12.3	3 058 000	50	872 300	3 007 000	48	1.18

[a] Calculated from average conversion determined by gravimetry and gas chromatography. [b] Calculated from M_n theory = ([BA]/[PBPEM]) × (molecular weight)$_{BA}$ × conversion. [c] Calculated from $DP_{n,SC-theory}$ = ([BA]/[PBPEM]) × conversion. [d] Determined by gel permeation chromatography in THF−conventional calibration with poly(methyl methacrylate) standards. [e] Determined by gel permeation chromatography in THF with a multiangle laser light scattering detector.

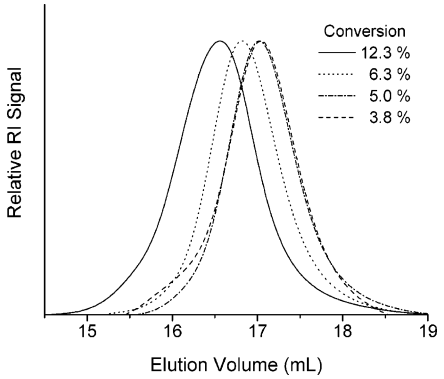

Figure 1. Gel permeation chromatography traces for the atom transfer radical polymerization of *n*-butyl acrylate (BA) (**B1**) with a poly(2-(2-bromopropionyl)oxyethyl methacrylate) (PBPEM) macroinitiator. [BA]:[R−Br]:[CuBr]:[$CuBr_2$]:[dNbpy] = 400:1:0.5:0.025:1, 70 °C, 4 vol % methyl ethyl ketone.

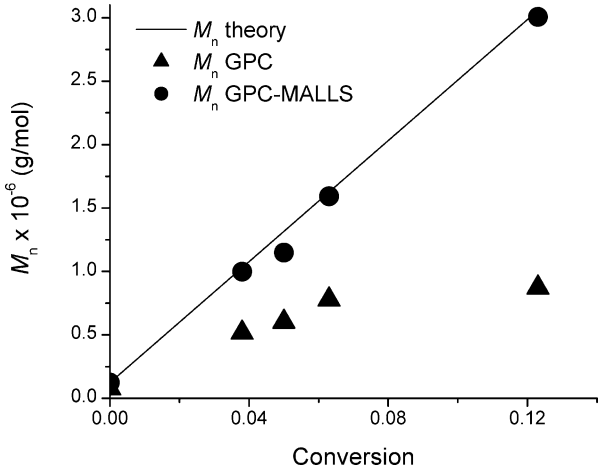

Figure 2. Molecular weight vs conversion for the polymerization of *n*-butyl acrylate (BA) (**B1**) with a poly(2-(2-bromopropionyl)oxyethyl methacrylate) (PBPEM) macroinitiator and [BA]:[R−Br]:[CuBr]:[$CuBr_2$]:[dNbpy] = 400:1:0.5:0.025:1, 70 °C, 4 vol % MEK. Molecular weights determined by gel permeation chromatography with a poly(methyl methacrylate) calibration (GPC) and multiangle laser light scattering detection (GPC-MALLS).

to provide well-defined brushes by grafting from via ATRP.[6,7] The polymerizations were essentially conducted in bulk BA with 4 vol % MEK included as an internal standard, and the [BA]:[PBPEM] ratio remained constant at 400:1. $CuBr_2$ was added initially to avoid its spontaneous generation by radical termination and to induce the persistent radical effect (PRE).[10,29−31] When synthesizing brushes by grafting from via a radical method, it is necessary to ensure a low concentration of active species due to the propensity of termination by both intra- and intermolecular coupling; therefore, the active species concentration was low, and moderate conversions were targeted. For comparison, BA was polymerized from both a PBPEM macroinitiator (brush polymerization, **B1**) and a low molecular weight ATRP initiator EtBrP (linear polymerization, **L1**). The extent of functionalization of the PBPEM macroinitiator was determined by ^{1}H NMR spectroscopy to be greater than 97%.

Evidence for the controlled nature of the polymerization of BA from a PBPEM backbone (**B1**) was obtained by GPC (Figure 1). A decrease in elution volume with increasing conversion is observed, which is qualitatively indicative of the molecular weight increasing throughout the polymerization. The traces are unimodal and show no indications of low molecular weight tailing or significant intermolecular termination. Molecular weights for the brushes were calculated by both conventional calibration vs PMMA standards and by MALLS detection (Table 2).

A linear relationship existed between the M_n values determined by GPC-MALLS and conversion (Figure 2). These values are undoubtedly more reliable than those obtained by conventional calibration since linear standards underestimate the true molecular weights for

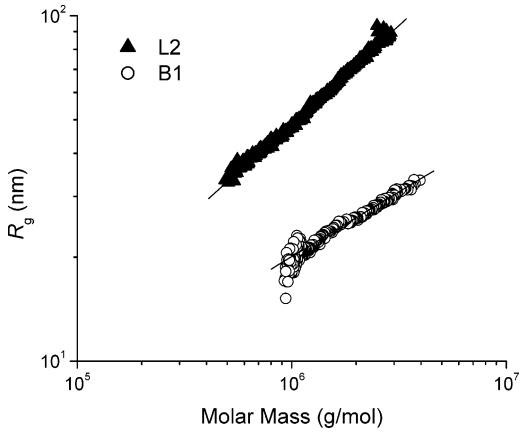

Figure 3. Radius of gyration (R_g) vs molar mass for linear poly(*n*-butyl acrylate) and poly(2-(2-bromopropionyl)oxyethyl methacrylate-*graft*-*n*-butyl acrylate) as determined by gel permeation chromatography with multiangle laser light scattering detection.

highly branched polymers. This is due to conventional GPC calibrations being based on hydrodynamic volume as compared to MALLS which provides absolute molecular weights. The difference can be elucidated by comparing the relationship between the size of a polymer in solution and its molecular weight for linear and highly branched structures.[32] Figure 3 demonstrates the difference in the radius of gyration (R_g) between a linear (**L2**) and a brush polymer (**B1**) of BA as determined by

Table 3. Results from the Side Chains Cleaved from the Poly(2-(2-bromopropionyloxy)ethyl methacrylate-*graft*-*n*-butyl acrylate) (P(BPEM-*graft*-BA)) Brushes in Order To Investigate Initiation Efficiency as a Function of Conversion

time (h)	conv[a] (%)	$M_{n,SC-theory}$[b]	$M_{n,SC-cleaved}$[c]	$DP_{n,SC-theory}$[d]	$DP_{n,SC-cleaved}$[e]	PDI_{SC}[c]	f[f] (%)
5	1.0	500					
20	3.8	1900	4200	15	33	1.17	45
22	5.0	2600	4900	20	38	1.18	53
26	6.3	3200	5400	25	43	1.24	58
47	12.3	6300	7100	48	55	1.37	87

[a] Calculated from average conversion determined by gravimetry and gas chromatography. [b] Calculated from $M_{n,SC-theory} = (M_{n,brush} - M_{n,PBPEM})/DP_{n,PBPEM}$. [c] Determined by gel permeation chromatography in THF with poly(*n*-butyl acrylate) calibration. [d] Calculated from $DP_{n,SC-theory} = (M_{n,SC-theory})/(\text{molecular weight})_{BA}$. [e] Calculated from $DP_{n,SC} = M_{n,SC}/(\text{molecular weight})_{BA}$. [f] Initiation efficiency calculated from eq 2.

Scheme 2. Outline for the Cleavage of Poly(*n*-butyl acrylate) (PBA) Side Chains from Poly(2-(2-bromopropionyloxy)ethyl methacrylate-*graft*-*n*-butyl acrylate) (P(BPEM-*graft*-BA)) Molecular Brushes

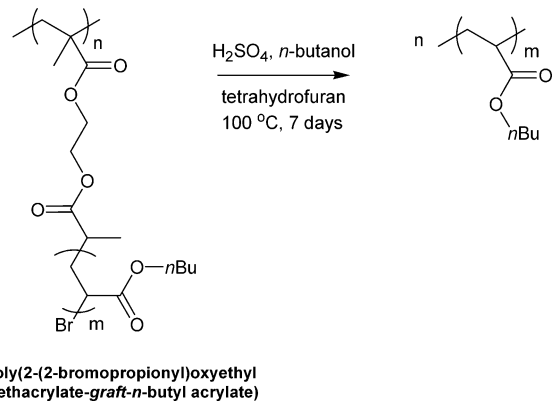

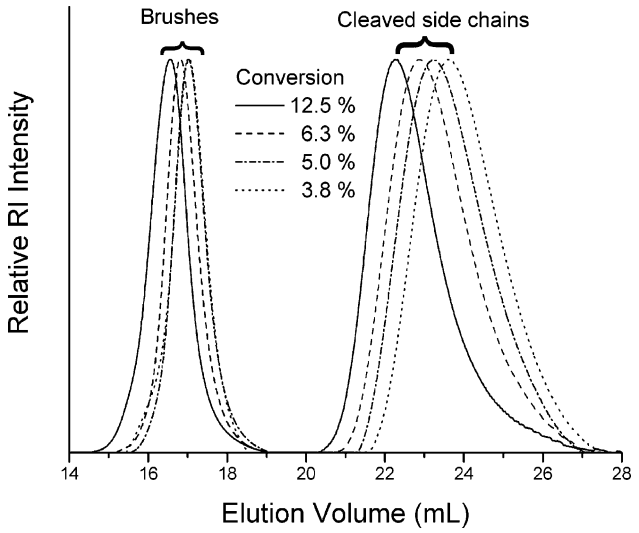

Figure 4. Gel permeation chromatography traces for poly(2-(2-bromopropionyl)oxyethyl methacrylate-*graft*-*n*-butyl acrylate) and the corresponding cleaved side chains at various levels of monomer conversion in polymerization **B1**.

MALLS. At a given molecular weight, R_g is significantly lower for **B1**. This is a quantitative indication of the inadequacy of conventional standards for the characterization of molecular brushes by GPC. Typical values for the slope of this plot for linear random coils are between 0.5 and 0.6, with lower values indicating branching.[33] The slopes for **L2** and **B1** samples were determined to be 0.58 and 0.36, respectively.

While analysis of the brush polymers can give an indication of the controlled nature of brush formation, direct analysis of the SCs is necessary to determine more information about the initiation efficiency of the polymerization. To obtain well-defined brushes, individual SCs should be of equal length. This requires the rate of initiation being fast with respect to the rate of propagation, thereby facilitating high initiation efficiency early in the polymerization so that all SCs begin growing simultaneously. To probe the initiation process for the brush synthesis, parallel reactions were conducted and stopped at different levels of conversion. The resulting SCs were cleaved by acid solvolysis in 1-butanol at 100 °C (Scheme 2). It has been previously demonstrated that complete cleavage of the SCs occurs under these conditions and that the identity of the ester functionalities of each monomer unit is preserved.[7] The polymers obtained from the cleavage reactions were then characterized by GPC to examine the growth of the SCs with monomer conversion (Figure 4). Following the solvolysis reactions, only low molecular weight polymer was observed, which indicates the cleavage reaction was nearly quantitative. Because the PBPEM backbone makes up a low percentage of the overall mass of the brush polymer, it is undetectable after the SCs are removed. Molecular weights for the cleavage products were calculated using a conventional calibration based on linear PBA standards (Table 3).

Assuming quantitative initiation, the theoretical molecular weight for the SCs ($M_{n,SC-theory}$) can be calculated according to eq 1

$$M_{n,SC-theory} = \frac{M_{n,brush} - M_{n,backbone}}{DP_{n,backbone}} \quad (1)$$

where $M_{n,brush}$ and $M_{n,backbone}$ are the number-average molecular weights of the brush and backbone, respectively, and $DP_{n,backbone}$ is the number-average degree of polymerization of the backbone. As mentioned previously, approximately 3% of the PBPEM backbone was incapable of initiating polymerization. This amount should be insignificant relative to the limited grafting efficiencies observed. Figure 5 shows the evolution of molecular weight vs conversion for **L1** and the cleaved SCs of **B1**. While the molecular weights (based on PBA standards) for both polymerizations deviate from theory at low conversions, the molecular weights from **L1** quickly approach the theoretical values while those from the **B1** continue to increase before approaching the theoretical line. This behavior is typical for systems demonstrating slow initiation with respect to propagation.

The comparison of **L1** and **B1** suggests the deviation from theoretical molecular weight for the brush polymerization can be attributed to steric congestion. Because of the relatively high propagation rate coefficient for BA,[34] each activation−deactivation cycle allows a significant number of monomers to be added to the newly formed radical center. In a typical ATRP employing a

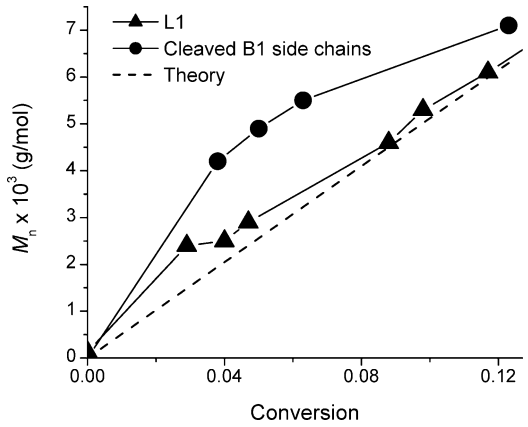

Figure 5. Evolution of molecular weight as a function of conversion for **L1** and the cleaved side chains from **B1**. [*n*-Butyl acrylate]:[R−Br]:[CuBr]:[$CuBr_2$]:[dNbpy] = 400:1:0.5:0.025:1, 70 °C, 4 vol % methyl ethyl ketone. Molecular weights determined by gel permeation chromatography with a conventional calibration based on poly(*n*-butyl acrylate) standards.

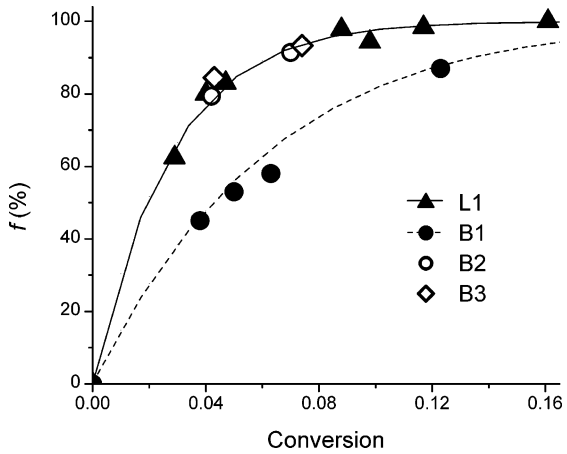

Figure 6. Initiation efficiency as a function of conversion for the brush (**B1**−**3**) and linear (**L1**) polymerizations of *n*-butyl acrylate. The solid and broken lines represent the fit of eq 4 to the data of **L1** and **B1**, respectively.

low molecular weight initiator, BA is polymerized in a controlled manner since several activation−deactivation cycles occur, and the large majority of the chains are dormant at any instant. This facilitates all chains growing to approximately equal lengths after a given period of time. When ATRP is employed for the preparation of molecular brushes, there is a high local concentration of initiation sites along the macroinitiator backbone. It is important that deactivation occurs quickly to prevent the SCs initiated first from growing to a degree that may prevent fast initiation at adjacent sites due to steric hindrance, limiting access of the initiation site to the catalyst complex and monomer. Nonetheless, while this phenomenon may cause the rate of initiation at the other sites to be significantly reduced, it does not prevent initiation completely, and nearly all sites eventually have SCs attached. This can be further supported by observing the initiation efficiency (f) as a function of conversion (Figure 6), where f is given by eq 2.

$$f = \frac{M_{n,SC-theory}}{M_{n,SC-cleaved}} \tag{2}$$

While f is initially low, it gradually increases with conversion for both **L1** and **B1**. The limited efficiency for the linear polymerization is due to a portion of the chains growing very rapidly due to the relatively high k_p of BA[34] as compared to the rate of deactivation (i.e., a product of the rate constant of deactivation, k_{da}, and the concentration of deactivator, Cu^{II}). However, at approximately 8% conversion, f approaches unity, and it can be assumed that nearly all initiating centers have grown to a significant extent. Similar behavior is observed for the brush polymerization with the difference being the extent of conversion required to reach quantitative initiation. In this case, the initiation efficiency is 45% at 3.8% monomer conversion, reaching nearly 90% at 12.5% conversion. The comparison of the results between the two systems supports the notion that congestion in the case of the brushes retards the initial chain growth from a portion of the initiation sites.

Litvinenko and Mueller[35] originally proposed that the fraction of residual initiator ($[I]/[I]_0$) for polymerizations with a rapidly reached equilibrium between species of different reactivity and a constant concentration of activator and deactivator (steady-state) can be defined as

$$\frac{[I]}{[I]_0} \approx (1-\alpha)(1-x)^{\beta} \exp(-\lambda\gamma^* x) \tag{3}$$

where α is the equilibrium fraction of more active species, x is the monomer conversion, λ is the ratio of rate constants for the propagation of less and more active species, $\gamma^* = ([M]_0/[I]_0)/[\alpha + \lambda(1-\alpha)]$, and

$$\beta = \frac{k_{da}[DA]}{k_p[I]_0(1-\alpha)} \frac{\alpha}{\alpha + \lambda(1-\alpha)} \tag{4}$$

where [DA] is the concentration of deactivator.

For ATRP, less active (i.e., dormant) chains predominate ($\alpha \approx 0$) and are incapable of propagating ($\lambda = 0$). It can also be assumed that reactivity is independent of chain length, which has been previously demonstrated by investigating the penultimate effects on the rate coefficient of activation (k_a) for the ATRP of acrylates.[36] Similarly, a steady-state radical concentration should be quickly established since the 2-bromopropionate initiating moieties and the dormant side chains are activated at approximately the same rate. These assumptions allow eq 3 to be simplified for ATRP, yielding

$$\frac{[I]}{[I]_0} = (1-x)^{k_{da}[DA]/k_p[I]_0} \tag{5}$$

Since $[I]/[I]_0$ is the fraction of residual initiator, the initiation efficiency can be described by

$$f = 1 - (1-x)^{k_{da}[DA]_0/k_p[I]_0} \tag{6}$$

Souaille and Fischer proposed a similar relationship describing f for polymerizations in which [DA] varies.[37] In the current study, the deactivator, $CuBr_2$, was present at the beginning of the polymerization, and its concentration should essentially be constant since it is not significantly affected by the PRE. By expressing f as a function of conversion instead of time, we can avoid variation that may arise from a slight induction period caused by adventitious impurities, incomplete removal of oxygen, etc.

For the ATRP of BA at 70 °C, $k_p = 4.0 \times 10^4$ L mol^{-1} s^{-1}.[34] Thus, by fitting the dependence of f with conversion according to eq 6 and knowing the concentrations of $CuBr_2$/dNbpy and initiation sites, k_{da} can be estimated as 6.1×10^7 L mol^{-1} s^{-1} for **L1** (Figure 6). Using the same method, k_{da} for **B1** is estimated to be 2.7×10^7 L mol^{-1} s^{-1}. This assumes that k_p is constant for **L1** and **B1**, which is likely since the polymerizations are conducted in bulk monomer, and as a result, steric congestion caused by newly formed SCs in the vicinity of the macroinitiator backbone is not expected to exclude the solvating monomer. The difference in k_{da} for **L1** and **B1** is consistent with increased steric congestion in the brush syntheses, leading to slower deactivation by the $CuBr_2$/dNbpy complex. This corroborates theoretical predictions that a difference in β by a factor of approximately 2 can have a significant effect on the initiation efficiency observed at low conversion in ATRP. Slow deactivation allows the chains initiated at low conversion to grow to lengths greater than that predicted by $DP_{n,SC-theory} = [BA]_0 x/[BPEM\text{-}Br]_0$, and as a result, $f = DP_{n,SC-theory}/DP_{n,SC}$ is lower than for the ideal case.

Two approaches were employed with the goal of reducing the number of monomers incorporated per activation−deactivation cycle: increasing the concentration of Cu^{II} (**B2**) and decreasing the monomer concentration (**B3**). Either of these methods should counterbalance the effect of slow deactivation and prevent the chains initiated first from reaching the lengths necessary to significantly interfere with adjacent initiation sites.

For understanding the approach used in polymerization **B2**, it is helpful to consider the rate law for copper-mediated ATRP, which is given as follows:[28]

$$R_p = k_p[M][P^\bullet] = k_p k_a k_{da}^{-1}[M][RX]_0 \frac{[Cu^I]}{[Cu^{II}]} \quad (7)$$

where [M] and [P•] are the concentrations of monomer and propagating radicals, respectively, $[RX]_0$ is the initial concentration of alkyl halide initiator, and k_a is the rate coefficient of activation. Therefore, when $[Cu^{II}]$ was increased in order to allow faster deactivation, it was necessary to simultaneously increase $[Cu^I]$ to maintain the same overall polymerization rate. In this manner, $[Cu^{II}]$:$[Cu^I]$ remains constant, but the window of time available for propagation is smaller; the chains that are initiated first grow to shorter lengths before being deactivated. For **B2**, the concentrations of Cu^I, Cu^{II}, and dNbpy were increased 5 times as compared to those employed in **B1** (Table 1). As expected, the apparent polymerization rate coefficient ($k_{app} = k_p[P^\bullet]$) did not change significantly with $k_{app} = 8.3 \times 10^{-7}$ s^{-1} being observed for **B2** as compared to $k_{app} = 8.0 \times 10^{-7}$ s^{-1} for **B1**. As seen in Figure 6, increasing the concentration of deactivator significantly improved the initiation efficiency of the brush polymerization to a level similar to that observed for the linear system.

For the second approach, the rate of propagation was decreased in order to reduce the number of propagation events per activation−deactivation cycle. This was accomplished with the amount of catalyst being the same as that employed in **B1**, but the monomer and initiator concentrations were halved by the addition of toluene (**B3**). The decreased initiator concentration caused the apparent rate coefficient to decrease ($k_{app} = 4.7 \times 10^{-7}$ s^{-1}) as expected, but this was accompanied by an expected increase in initiation efficiency. Following subsequent cleavage reactions, f was determined to be greater than 80% after only 4% conversion, and nearly 90% efficiency was obtained at 7% conversion (Figure 6). In fact, decreasing the initiator concentration by a factor of 2 caused the initiation efficiency of **B3** to be approximately equal to that observed for **L1** at a similar level of conversion. This is in excellent agreement with the prediction obtained using eq 4, since the exponential term is approximately double that of **B1** for both **L1** and **B3**. **B2** did not show similar agreement with eq 4, as evidenced by an increase in $[Cu^{II}]$ by a factor of 5, resulting in only an increase in the exponential term by a factor of approximately 2. This could be due to a higher than expected $[Cu^{II}]$ in **B1** that arises from the small portion of CuBr that spontaneously oxidized. Therefore, when an excess of $CuBr_2$ was added in **B3**, the actual increase in $[Cu^{II}]$ may not have been as significant as predicted. Additionally, as the number of monomer units incorporated per activation−deactivation cycle, $m = (k_p[M])/(k_{da}[Cu^{II}])$, approaches one, there is expected to be a reduced dependence of increased deactivator concentration on f. Regardless, increasing the rate of deactivation or decreasing the rate of propagation proved to be sufficient means of increasing the initiation efficiency to a level approaching those obtained with typical linear ATRP reactions. In principle, the same approach can be used for other systems with inefficient initiation for rapidly propagating monomers.

Conclusions

Initiation in the grafting from polymerization of BA from a PBPEM backbone is not quantitative at low conversion. In contrast, more efficient initiation was observed at low conversion for an analogous linear polymerization conducted under identical conditions except that a low molecular weight initiator was employed. Comparison of the two indicates that the initiation/grafting efficiency for the synthesis of molecular brushes is affected by the inherent high density of initiation sites, which causes slower deactivation as compared to the linear polymerization. The SCs that begin growing early at a fraction of the initiation sites sterically hinder adjacent backbone repeat units, causing noncomplete initiation at low conversion. By analyzing the cleaved SCs, the initiation/grafting efficiency was shown to increase with conversion. Decreasing the number of propagation events that occur before deactivation proved to be a viable method of increasing the initiation efficiency. This was accomplished by either increasing the concentration of Cu^{II} or reducing the concentration of monomer.

Because many of the properties of molecular brushes are dependent on the density of grafting and because it is often necessary to target low conversion in order to prepare brushes with short SCs, it is important to gain further understanding of the factors affecting initiation during grafting from via ATRP. These findings not only may be important for the synthesis of molecular brushes but also may provide insight into other polymerizations systems in which initiation occurs in sterically confined environments (core first star syntheses, grafting from flat surfaces or colloids, etc.).

Acknowledgment. This work was financially supported by the National Science Foundation (ECS 01-

03307 and CHE 01-30903) and the CRP Consortium at CMU. The authors also thank Jinyu Huang for synthesizing the high molecular weight PBA.

References and Notes

(1) Bhattacharya, A.; Misra, B. N. *Prog. Polym. Sci.* **2004**, *29*, 767−814.
(2) Fischer, K.; Schmidt, M. *Macromol. Rapid Commun.* **2001**, *22*, 787−791.
(3) Neugebauer, D.; Zhang, Y.; Pakula, T.; Sheiko, S. S.; Matyjaszewski, K. *Macromolecules* **2003**, *36*, 6746.
(4) Cheng, G.; Boeker, A.; Zhang, M.; Krausch, G.; Mueller, A. H. E. *Macromolecules* **2001**, *34*, 6883−6888.
(5) Mori, H.; Mueller, A. H. E. *Prog. Polym. Sci.* **2003**, *28*, 1403−1439.
(6) Beers, K. L.; Gaynor, S. G.; Matyjaszewski, K.; Sheiko, S. S.; Moeller, M. *Macromolecules* **1998**, *31*, 9413−9415.
(7) Boerner, H. G.; Beers, K.; Matyjaszewski, K.; Sheiko, S. S.; Moeller, M. *Macromolecules* **2001**, *34*, 4375−4383.
(8) Boerner, H. G.; Duran, D.; Matyjaszewski, K.; da Silva, M.; Sheiko, S. S. *Macromolecules* **2002**, *35*, 3387−3394.
(9) Qin, S.; Matyjaszewski, K.; Xu, H.; Sheiko, S. S. *Macromolecules* **2003**, *36*, 605−612.
(10) Matyjaszewski, K.; Qin, S.; Boyce, J. R.; Shirvanyants, D.; Sheiko, S. S. *Macromolecules* **2003**, *36*, 1843−1849.
(11) Neugebauer, D.; Zhang, Y.; Pakula, T.; Matyjaszewski, K. *Polymer* **2003**, *44*, 6863−6871.
(12) Zhang, W.; Zhang, X. *Prog. Polym. Sci.* **2003**, *28*, 1271−1295.
(13) Fredrickson, G. H. *Macromolecules* **1993**, *26*, 2825.
(14) Subbotin, A.; Saariaho, M.; Ikkala, O.; Brinke, G. t. *Macromolecules* **2000**, *33*, 3447.
(15) Hsieh, H. L.; Quirk, R. *Anionic Polymerization. Principle and Practical Applications*; Dekker: New York, 1996.
(16) Muchtar, Z.; Schappacher, M.; Deffieux, A. *Macromolecules* **2001**, *34*, 7595−7600.
(17) Wintermantel, M.; Gerle, M.; Fischer, K.; Schmidt, M.; Wataoka, I.; Urakawa, H.; Kajiwara, K.; Tsukahara, Y. *Macromolecules* **1996**, *29*, 978−983.
(18) Yamada, K.; Miyazaki, M.; Ohno, K.; Fukuda, T.; Minoda, M. *Macromolecules* **1999**, *32*, 290−293.
(19) Schappacher, M.; Deffieux, A.; Putaux, J.-L.; Viville, P.; Lazzaroni, R. *Macromolecules* **2003**, *36*, 5776−5783.
(20) Tsukahara, Y.; Inoue, J.; Ohta, Y.; Kohjiya, S.; Okamoto, Y. *Polym. J. (Tokyo)* **1994**, *26*, 1013.
(21) Baskaran, D. *Prog. Polym. Sci.* **2003**, *28*, 521−581.
(22) Tsukahara, Y.; Tsutsumi, K.; Yamashita, Y.; Shimada, S. *Macromolecules* **1990**, *23*, 5201.
(23) Breunig, S.; Heroguez, V.; Gnanou, Y.; Fontanille, M. *Macromol. Symp.* **1995**, *95*, 151−166.
(24) Heroguez, V.; Breunig, S.; Gnanou, Y.; Fontanille, M. *Macromolecules* **1996**, *29*, 4459.
(25) Matyjaszewski, K.; Xia, J. *Chem. Rev.* **2001**, *101*, 2921−2990.
(26) Kamigaito, M.; Ando, T.; Sawamoto, M. *Chem. Rev.* **2001**, *101*, 3689−3745.
(27) Goto, A.; Fukuda, T. *Prog. Polym. Sci.* **2004**, *29*, 329−385.
(28) Matyjaszewski, K.; Patten, T. E.; Xia, J. *J. Am. Chem. Soc.* **1997**, *119*, 674−680.
(29) Fischer, H. *Macromolecules* **1997**, *30*, 5666−5672.
(30) Davis, K. A.; Paik, H.-j.; Matyjaszewski, K. *Macromolecules* **1999**, *32*, 1767−1776.
(31) Shipp, D. A.; Matyjaszewski, K. *Macromolecules* **2000**, *33*, 1553−1559.
(32) Zimm, B. H.; Stockmayer, W. H. *J. Chem. Phys.* **1949**, *17*, 1301−1314.
(33) Podzimek, S.; Vlcek, T. *J. Appl. Polym. Sci.* **2001**, *82*, 454−460.
(34) Beuermann, S.; Buback, M. *Prog. Polym. Sci.* **2002**, *27*, 191−254.
(35) Litvinenko, G.; Mueller, A. H. E. *Macromolecules* **1997**, *30*, 1253−1266.
(36) Nanda, A. K.; Matyjaszewski, K. *Macromolecules* **2003**, *36*, 8222−8224.
(37) Souaille, M.; Fischer, H. *Macromolecules* **2002**, *35*, 248−261.

MA048351B